

---

# Program for PET Image Alignment: Effects on Calculated Differences in Cerebral Metabolic Rates for Glucose

Robert L. Phillips, Edythe D. London, Jonathan M. Links, and Nicola G. Cascella

*Neuropharmacology Laboratory, Addiction Research Center, National Institute on Drug Abuse, Baltimore, Maryland and Division of Nuclear Medicine, The Johns Hopkins Medical Institutions, Baltimore, Maryland*

---

A program was developed to align positron emission tomography images from multiple studies on the same subject. The program allowed alignment of two images with a fineness of one-tenth the width of a pixel. The indications and effects of misalignment were assessed in eight subjects from a placebo-controlled double-blind crossover study on the effects of cocaine on regional cerebral metabolic rates for glucose. Visual examination of a difference image provided a sensitive and accurate tool for assessing image alignment. Image alignment within 2.8 mm was essential to reduce variability of measured cerebral metabolic rates for glucose. Misalignment by this amount introduced errors on the order of 20% in the computed metabolic rate for glucose. These errors propagate to the difference between metabolic rates for a subject measured in basal versus perturbed states.

**J Nucl Med 1990; 31:2052-2057**

---

The need to align images obtained by positron emission tomography (PET) arises frequently. A repeated measurement paradigm is often used with this imaging modality, and images from repeated studies must be aligned for comparison. Such a paradigm has been used to assess acute effects of many perturbations, including the administration of psychoactive substances, such as barbiturates (1), morphine (2), and alcohol (3). It also has been used to infer changes in neuronal function due to cognitive tasks (4). In addition, studies on the progress of chronic pathologic conditions, such as Alzheimer's disease (5), acquired immunodeficiency syndrome (AIDS) (6), and cancer (7), have used this approach.

In a repeated measurement paradigm, each subject is his own control. A change in functional activity is inferred from the change in radioactivity (or the corresponding metabolic rate) in a subregion of an anatomic

structure or in the whole brain. Since the activity distribution over the structure of interest may be heterogeneous, it is important to sample the same anatomic site in both the test and the retest studies. Even the best human-use head holders cannot completely eliminate head motion and misalignment (8). Therefore, some means of detection or, preferably, correction for this motion is necessary.

We have developed methodology for alignment of images from multiple PET studies. Our method reduces artifacts in the regional measurements due to movement of the subject between serial scans. We have assessed the magnitude of spurious effects due to small (<2.8 mm) differences in locating regions of interest (ROIs) in the image. The data examined in this report were obtained in PET studies using [fluorine-18]fluorodeoxyglucose (FDG) to measure regional cerebral metabolic rate(s) for glucose ( $rCMR_{glc}$ ). The method is equally applicable to PET studies employing other imaging agents.

## MATERIALS AND METHODS

### Subjects

Eight subjects were recruited into a study on the effects of cocaine on  $rCMR_{glc}$  (9). The study was a collaborative effort of the NIDA Addiction Research Center (located at The Francis Scott Key Medical Center) and the Division of Nuclear Medicine of The Johns Hopkins Medical Institutions. The institutional review boards of The Francis Scott Key Medical Center and The Johns Hopkins Medical Institutions both approved the protocol. All subjects were polydrug abusers with a recent history of intravenous cocaine use. They gave informed consent prior to the studies.

### PET Scans

All eight subjects first received an X-ray computed tomography (CT) scan. Images acquired by CT were parallel to and elevated from the inferior orbitomeatal (IOM) plane (Reid's base line) by 16-112 mm in 8-mm steps. Marking these planes on a thermoplastic face mask, molded individually for each subject, formed a reference for alignment of CT and PET scans. The mask also was used to immobilize the subject's head during CT and PET data acquisition. Procedural controls

---

Received Dec. 27, 1989; revision accepted May 10, 1990.  
For reprints contact: Dr. Robert L. Phillips, NIDA Addiction Research Center, P.O. Box 5180, Baltimore, MD 21224.

to minimize variability in the data included administration of a standardized non-ketogenic breakfast followed by fasting until after the scan, and standardization of scanning time to the early afternoon (13:00 to 15:00) to minimize diurnal effects (10). The test compound (placebo or cocaine) was administered double-blind in a random sequence to minimize effects of anticipation (11). Subjects were studied at rest (except for the intermittent reporting of their feeling state) rather than while performing a complex task (12).

The NeuroECAT PET tomograph (CTI, Knoxville, TN) was used in these studies. This scanner simultaneously acquires 3 planes on 32-mm centers. Four plane sets were acquired over a 60-min period to yield 12 images on 8-mm centers. Although head position was almost continuously monitored, this length of time was enough to provide an opportunity for the subject to move his head by several millimeters between scans. In addition, the two studies were separated by 48 hr or more; so that the subject had to be repositioned in the scanner for the second study.

The data set for each PET study consisted of 12 files. Each of the files contained a  $100 \times 100$  integer array with the "reconstructed counts" from the PET scan. These "ECAT numbers" were corrected for attenuation, using a separate, operator-defined ellipse around the brain on each slice. The ellipse was also used for preliminary rotation and shift alignment of the image of the brain within the matrix. This alignment was actually performed during the backprojection step on the projection data. The ellipse in-plane rotation alignment was in integral angular steps of  $2.04^\circ$ . Translations were done in increments of 2.85 mm. The data set was then transferred via magnetic tape to a commercial PET analysis system (Loats Assoc., Westminster, MD). The system uses the equation of Huang et al (13), including correction for finite clearance of  $^{18}\text{F}$ FDG, as the primary operational equation to convert ECAT numbers to  $\text{rCMR}_{\text{glc}}$ .

The films from the CT scan were used to determine the most representative slices for locating 50 standardized anatomical ROIs in the PET scans. A rectangular box was placed near the center of each brain region. The placement of ROIs in the first study was also performed using the Loats PET system. The boxes had dimensions of  $4 \times 4$  pixels (1 pixel = 2.8 mm) for cortical structures and  $3 \times 3$  or  $3 \times 4$  pixels for interior structures. One region (the gyrus rectus) was sampled with a  $5 \times 10$  pixel ROI. When placing ROIs and analyzing the data, the reader was blinded to the treatment condition (placebo or cocaine).

### Alignment Program

The alignment program was written in Microsoft C (Microsoft Corp, Redwood, WA) and is designed to operate on an  $80 \times 86$  based computer (Intel Corp, Hillsboro, OR) under Microsoft DOS. It has been tested and used on COMPAQ 386/20 and AST 386C computers with VGA adapters and monitors. It uses the medium resolution mode of the VGA (i.e., 256 colors and  $320 \times 200$  pixels). Any PC-AT compatible computer with VGA adapter should run the program without modifications. Conversion to other computer types should be facilitated by the extensive use of ANSI standard routines, except for graphics primitives (which are part of the MS C graphical interface). Machine language was deliberately not used in order to facilitate portability of the code.

The program assumes that the data for each plane in the 12 element plane set is composed of a  $100 \times 100$  pixel array of data values for each plane. This format is the standard presentation for images produced by the NeuroECAT tomograph and the Loats PET analysis system. Provision was made for changing these dimensions to accommodate data from other scanners.

### Alignment Algorithm

Assessment of image alignment was based primarily on visual inspection of a "difference image," formed by subtraction of the second from the first study. The second image could be iteratively translated with respect to the first, until the best visual alignment was achieved.

Two mechanisms were used for image translation. For translations by whole pixel lengths, the image array was simply translated pixel-for-pixel, with end points of the image replicated. This approach preserved all information in the central region of the image, and was appropriate for gross alignment.

A two-dimensional linear interpolation algorithm was used for finer adjustments. This calculation was given by:

$$C_{(x+\delta x, y+\delta y)} = C_{(x+\delta x, y)} + \delta y \times \{C_{(x+\delta x, y+1)} - C_{(x+\delta x, y)}\}$$

with:

$$C_{(x+\delta x, y)} = C_{(x, y)} + \delta x \times \{C_{(x+1, y)} - C_{(x, y)}\}$$

$$C_{(x+\delta x, y+1)} = C_{(x, y+1)} + \delta x \times \{C_{(x+1, y+1)} - C_{(x, y+1)}\},$$

where  $0 \leq \delta x < 1$ ,  $0 \leq \delta y < 1$  were the fractional part of the shift in the  $x$  and  $y$  directions respectively, and  $C_{(x, y)}$  was the  $\text{rCMR}_{\text{glc}}$  at pixel  $(x, y)$ .

The program used 0.1 pixel steps, but such precision was rarely required or detectable in practice, as it was usually not possible to resolve motion finer than 0.2 pixels. These dimensions were specific to the NeuroECAT scanner; it is probable that smaller shifts could be resolved with data from a scanner with higher intrinsic resolution.

Figure 1 shows the screen display used by the operator. The actual display shows the images in color using gradations of intensity of blue for positive differences and red for negative differences with near black shades for small differences. This

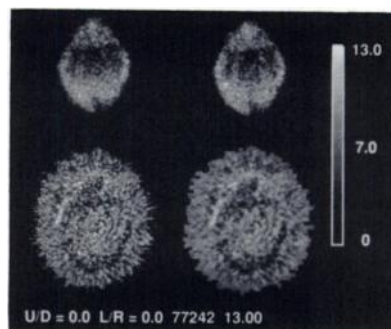


**FIGURE 1**  
Simulation of operator's display from the alignment program. The two upper images show  $\text{rCMR}_{\text{glc}}$  from the first and second PET study on the left and right, respectively. The lower images show the raw and smoothed difference images (left and right, respectively) formed by subtracting the top right image from the top left image. The units for this and all other figures are  $\text{mg}/100 \text{ g}/\text{min}$ . The scale is from 0 to 13 for the top images and  $-5$  to  $+5$  for the difference images.

color scale facilitates observation of the halo artifacts, which characterize positional discrepancies. The top left image shows the first of two scans. The top right shows the second scan. The lower left image is the raw difference image. The image on the lower right has been smoothed using the following convolution kernel:

$$\begin{vmatrix} 1 & 2 & 1 \\ 2 & 4 & 2 \\ 1 & 2 & 1 \end{vmatrix}$$

The unsmoothed image was usually dominated by high frequency noise, while the smoothed image better portrayed artifacts due to misalignment. The text on the bottom reports the magnitude of shift (in 0.1 pixel units), the scaled sum of squared differences between the first and second images and the maximum value of  $rCMR_{glc}$  in the images. The operator could iteratively shift one image with respect to the other in 0.1-pixel increments until the artifacts in the difference images and/or the sum of squared differences were minimized.

### RESULTS

Figures 2 thru 5 show effects of alignment. The slice shown in these figures is ~32 mm above the IOM plane. It was chosen for illustrative purposes because it contains structures in the cortex (superior, medial, and inferior temporal gyri), closer to the centerline (amygdala, hippocampus, and parahippocampus), and on the centerline (gyrus rectus).

Figures 2 and 3 show the effect of misaligning the images by one pixel horizontally and/or vertically. The corner images are displaced by 1.4 pixels (3.9 mm). In Figure 2, we show a series of nine difference images. The correct alignment is shown in the center. Note the appearance of "halos" in the misaligned images. These arcs represent "edge artifacts," whose pattern indicates the direction of misalignment. Figure 3 shows smoothed difference images. Note that smoothing reduces the random statistical noise "background," improving perception of the halos.

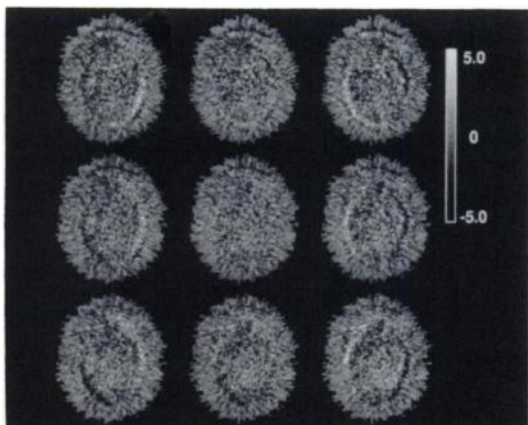


**FIGURE 2**  
Effect of image misalignment. Note the artifacts produced by shifting the image from the second study by one pixel (2.8 mm) in eight directions from correct alignment. The artifacts are composed of partial halos with the outermost white halo pointed in the direction of the shift required to align the image.

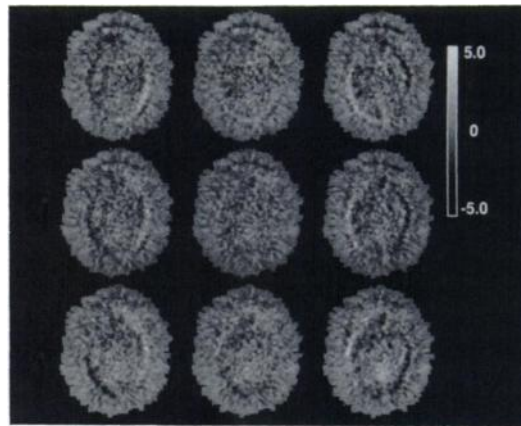


**FIGURE 3**  
Effect of image misalignment. The same images shown in Figure 1 but smoothed with the convolution kernel given in the text. Note that the halos are more pronounced and easier to see.

Figures 4 and 5 show the same planes but use half pixel misalignment. Notice that halos are still visible, but less obvious than with whole pixel misalignment. These images relate to those of Figures 2 and 3 as being at the intersection of each four corner images. Figure 6 illustrates the placement of ROIs on the raw images. There is little to indicate the discrepancy in placement on image #2. Figure 7, on the other hand, shows the difference and smoothed difference images for the initial and aligned configuration. The effects of misalignment can be surmised from the location of the "halo" artifacts. The lack of halo artifacts is characteristic and can be produced with nearly all pairs of images studied to date.

The average magnitude of shift used for all 59 analyzed planes from the eight subjects was  $0.802 \pm 0.52$  (mean  $\pm$  s.d.) pixels. For a given subject, the correlation of the shifts from slice to slice was governed by the two sources of misalignment:

1. The head was identically oriented for the first and second scan, but orthogonally translated with re-

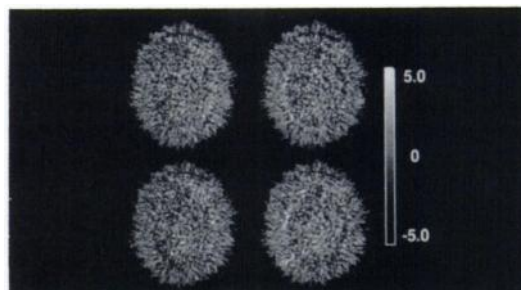


**FIGURE 4**  
Effect of 0.5 pixel misalignment. These images are offset from the aligned image (shown in the center of Fig. 1) by half a pixel (1.4 mm) (total shift 2 mm) in the four diagonal directions. Note that the white halos are in similar positions to those of the corner images in Figure 1 but they are less pronounced.

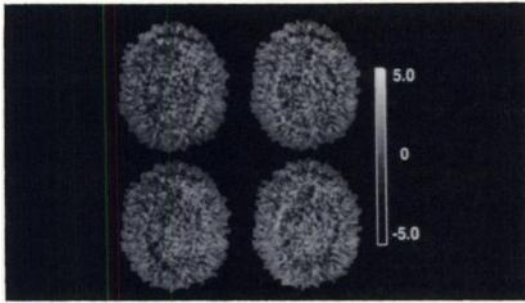


**FIGURE 5**  
Effect of 0.5 pixel misalignment in smoothed images. These images are offset from the aligned image (center image in Fig. 2) by half a pixel (1.4 mm) in the four diagonal directions. Note that the white halos are in similar positions to those of the corner images in Figure 2 but they are less pronounced.

spect to the scanner's axis. This misalignment produced a consistent shift across slices.

2. The head was tilted relative to the scanner's long axis. This misalignment required different magnitude and direction shifts from slice to slice, dependent on the degree of tilt and the location of the "pivot point."

Both of these sources of misalignment could occur at any time during acquisition of the four separate plane sets; both types of misalignment could, thus, be present in a given subject's 12 plane data set.

It is possible for the image to shift out-of-plane as well. In this case, the primary manifestation is the appearance of complete halos surrounding the outer contour of the brain and inner structures (e.g., the ventricles or cerebellum). Significant out-of-plane shifts did not occur in any of the plane sets analyzed in this study. The effects could easily be observed, however, by displaying a noncorresponding slice (from a different subject or slice within subject) as the second image.

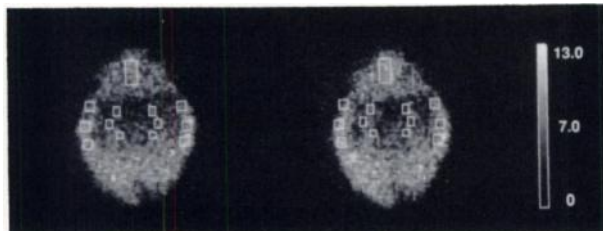


**FIGURE 6**  
The two slices with ROIs indicated by 13 white rectangles superimposed on the image. On the left, is the image taken from the study in the cocaine condition, the image on the right is from the study in the placebo condition. In this image, the ROIs were placed by an investigator (NGC) on the left image and the template was automatically placed on the right image. The outer six ROIs are (from top to bottom) the superior, medial, and inferior temporal gyri (left and right). At the top is the gyrus rectus ROI. The inner set of six ROIs sample (from top to bottom) the amygdala, hippocampus, and parahippocampus. The second image is offset from best alignment down 1.5 pixel and right 0.5 pixel.

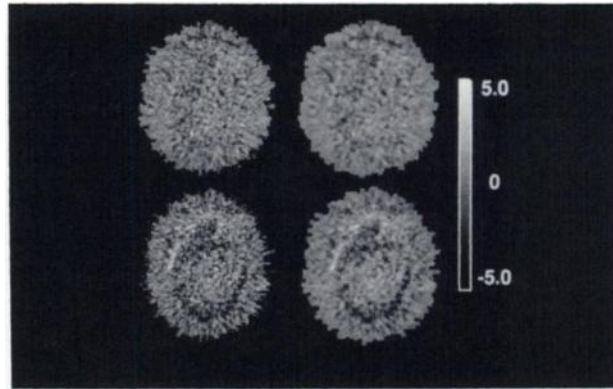


**FIGURE 7**  
Difference images from the slice illustrated in Figure 1. The top figures show the raw (left) and smoothed (right) difference images after proper alignment (up 1.5 pixel, left 0.5 pixel). The bottom row shows the raw and smoothed images from the original alignment.

The largest observed shift was 2.0 pixels, which occurred in two subjects. There was no "preferred" direction to the shift. The mean shift in the  $x$  direction was  $0.14 \pm 0.64$  pixels, and in the  $y$  direction it was  $0.10 \pm 0.74$  pixels. To illustrate the magnitude of the discrepancy possible with this shift, we show the range of  $rCMR_{glc}$  under shifts in the four "cardinal" directions (up, down, left and right) of one pixel in Figure 8. These are the results for seven subjects in four ROIs (left and right medial temporal gyrus and hippocampus). The quantity displayed is the percent difference between placebo and cocaine conditions:

$$200 \times \frac{rCMR_{glc}^C - rCMR_{glc}^P}{rCMR_{glc}^C + rCMR_{glc}^P}$$

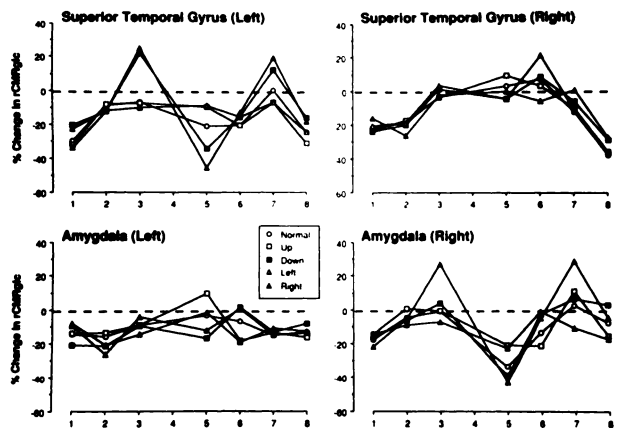


**FIGURE 8**  
Effect of image misalignment on calculation of  $rCMR_{glc}$ . The graphed quantity is percent differences in  $rCMR_{glc}$  from the placebo condition to the cocaine condition. Open circles describe the condition with the images at "best" alignment, boxes describe the data with the second study shifted up (open) or down (closed) by 1 pixel (2.8 mm). The triangles describe the calculation if the second study is shifted left (open) or right (closed) by 1 pixel (2.8 mm).

The slices used correspond to those shown in Figures 2–7. The first curve shows the calculated percent difference with the images aligned. The other four curves in each set show the effects on the calculated percent difference in  $rCMR_{glc}$  of displacing the ROI in the second study by one pixel (2.8 mm).

The magnitude of the discrepancy ranged from over 20% to less than 5%. It was highly dependent on the subject and ROI sampled. For example, in the superior temporal gyrus, Subject 3 showed changes from –10% for aligned, up, and left to +25% for motion of the second study down or right. Subject 5 showed –20% change for aligned, but –10% for up and left motion, and –30% to –40% for motion down or right. Figure 9 shows the magnitude of difference observed in all 50 ROIs for each subject. The quantity plotted is the difference between the shifted and unshifted  $rCMR_{glc}$ . The range markers show the maximum effects observed. These differences occurred in all regions and all subjects; they were not dependent on location within the slice, but existed throughout the brain.

## DISCUSSION

The need to align images obtained by PET arises frequently. A repeated measurement paradigm is often used with this imaging modality, and images from repeated studies must be aligned for comparison. Current methods for image alignment trace surface features of the brain (14) or rely on determination of “landmarks” in the anatomic image (15). These techniques offer positioning precision on the order of a few millimeters. In the proposed method, both of the above indicators of alignment are combined to register multiple PET images from the same subject.

The technique presented here uses an image formed by subtracting one image from the corresponding image in a pair representing repeated measures on the same tomographic slice. If there is a positional discrepancy

between the two original images, the difference image presents edge enhancements of all regions that differ significantly in activity from neighboring regions in the brain. The outer edge of the brain (the skull) determines the most easily visible edge enhancement, although the edges defined by the ventricles are visible and provide useful positioning information. In-plane motion can be detected and removed; out-of-plane motion can be detected but is not removed in the current paradigm.

Other methods exist for analyzing functional anatomical data without need for precise positioning. For example, centroids (16) can be used to determine changes in frontality and laterality. This technique, while insensitive to motion or misalignment of the subject between scans, does not identify anatomic structures with treatment-induced changes in activity. Change distribution techniques (17) require careful image alignment and do not directly distinguish structures that show changes due to the treatment perturbation from misalignment artifacts.

Corrections for positioning have been proposed previously. Many of these techniques rely upon stereotactic methods, where a specially designed frame is attached to the head. The images then contain data from this frame. The locations of the frame data in the scan image are used to mathematically warp the datasets into congruence (18). These techniques offer precision on the order of 3 mm. Others use an atlas of “normal” brain physiology (19). This technique has the disadvantage of ignoring the variability in brain morphology between subjects. Both techniques are valuable for alignment between imaging modalities and subjects. The cost incurred in using them is increased uncertainty in alignment within modality and within subject.

The use of whole slice difference images has been a useful paradigm for positioning PET images acquired from multiple studies on a single subject. Errors in positioning of the order of 0.5 pixel are clearly visible. Positioning discrepancies can be reduced to the order of 0.25 pixel. This correction can reduce the effects of misplacing ROIs. Without careful positioning, errors in differences on the order of 10%–20% are possible. Such errors are very pronounced in ROIs, such as those from the cortex, where  $rCMR_{glc}$  varies markedly between adjacent areas.

Further improvements to this methodology are expected from the use of newer generation tomographs, which can acquire complete plane sets in one scan. On the other hand, rotation of the subject’s head about any axis perpendicular to the z-axis would produce shifts in the image plane which would, in general, appear to be different at each plane. Such shifts are ideally suited for analysis by this method. In addition, the incorporation of rotational alignment would probably increase registration accuracy, although the rotation alignment performed during reconstruction in the present study ap-

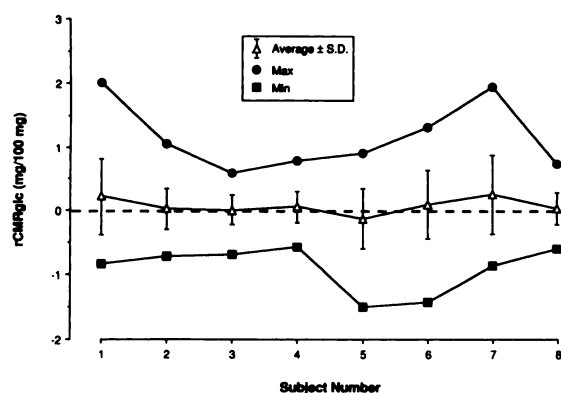


**FIGURE 9**  
Effect of image alignment. The plot shows the mean  $\pm$  s.d., maximum and minimum of the differences (aligned vs. unaligned) in  $rCMR_{glc}$  in all eight subjects for all ROIs.

peared adequate within the sampling resolution of the NeuroECAT.

Finally, this technique is not limited to use with FDG studies. The results of Mintun et al (4) show great similarity in the images acquired in matched control studies of cerebral blood flow using oxygen-15. Therefore, alignment by examination of difference images is a suitable method for eliminating motion artifacts in this paradigm.

## ACKNOWLEDGMENTS

The participation of JML in this research was supported in part by NIH grant NS15080. The authors acknowledge the assistance of Harry and Peter Loats and Bryan Kuyatt of Loats Associates for their help in interfacing this program to the Loats PET analysis system. The assistance of the Johns Hopkins Hospital nuclear medicine staff, particularly David Clough, CNMT, in acquiring the PET data is gratefully acknowledged.

## REFERENCES

1. Theodore WH, DiChiro G, Margolin R, Porter RJ, Fishbein D, Brooks RA. Barbiturates reduce human cerebral glucose metabolism. *Neurology* 1986; 36:60-64.
2. London ED, Broussolle EPM, Links JM, et al. Morphine-induced metabolic changes in human brain: studies with positron emission tomography and [fluorine-18] fluorodeoxyglucose. *Arch Gen Psychiat* 1990; 47:73-81.
3. Volkow ND, Mullani N, Gould L, et al. Effects of acute alcohol intoxication on cerebral blood flow measured with PET. *Psych Res* 1988; 24:201-209.
4. Mintun MA, Fox PT, Raichle ME. A highly accurate method of localizing regions of neuronal activation in the human brain with positron emission tomography. *J Cereb Blood Flow Metab* 1989; 9:96-103.
5. Foster NL, Chase TN, Fedio P, Patronas NJ, Brooks RA, DiChiro G. Alzheimers's disease: focal cortical changes shown by positron emission tomography. *Neurology* 1983; 33:961-965.
6. Brunetti A, Berg G, DiChiro G, et al. Reversal of brain metabolic abnormalities following treatment of AIDS dementia complex with 3'-azido-2',3'-dideoxythymidine (AZT, Zidovudine): a PET-FDG study. *J Nucl Med* 1989; 30:581-590.
7. Francavilla TL, Miletich RS, DiChiro G, Patronas NJ, Rizzoli HV, Wright DC. Positron emission tomography in the detection of malignant degeneration of low-grade gliomas. *Neurosurgery* 1989; 24:1-5.
8. Brooks RA, DiChiro G, Zukerberg BW, Bairamian D, Larson SM. Test-retest studies of cerebral glucose metabolism using fluorine-18 deoxyglucose: validation of method. *J Nucl Med* 1987; 28:53-59.
9. London ED, Cascella NG, Wong DF, et al. Cocaine-induced reduction of glucose utilization in human brain: a study using positron emission tomography and [fluorine-18]fluorodeoxyglucose. *Arch Gen Psychiatry* 1990; 47:567-574.
10. Bartlett EJ, Brodie JD, Wolf AP, Christman DR, Laska E, Meissner M. Reproducibility of cerebral glucose metabolic measurements in resting human subjects. *J Cereb Blood Flow Metab* 1988; 8:502-512.
11. Muntaner C, Cascella NG, Kumor KM, Nagoshi C, Herning R, Jaffe J. Placebo responses to cocaine administration in humans: effects of prior administration and verbal instructions. *Psychopharmacology* 1989; 99:282-286.
12. Duara R, Gross-Glenn K, Barker WW, Chang JY, Apicella A, Loewenstein D, Boothe T. Behavioral activation and the variability of cerebral glucose metabolic measurements. *J Cereb Blood Flow Metab* 1989; 7:266-271.
13. Huang SC, Phelps ME, Hoffman EJ, Sideris K, Selin CJ, Kuhl DE. Noninvasive determination of local cerebral metabolic rate of glucose utilization in man. *Am J Physiol* 1980; 238:E69-E82.
14. Pelizzari CA, Chen GTY, Spelbring DR, Weichselbaum RR, Chen CT. Accurate three-dimensional registration of CT, PET and/or MR images of the brain. *J Comput Assist Tomogr* 1989; 13:20-26.
15. Geckle WJ, Frank TL, Links JM, Becker LC. Correction for patient and organ movement in SPECT: applications to exercise thallium-201 cardiac imaging. *J Nucl Med* 1988; 29:441-450.
16. Levy AV, Brodie JD, Russell AG, Volkow ND, Laska E, Wolf AP. The metabolic centroid method for PET Brain Image Analysis. *J Cereb Blood Flow Metab* 1989; 9:388-397.
17. Fox PT, Mintun MA, Reiman EM, Raichle ME. Enhanced detection of focal brain responses using intersubject averaging and change-distribution analysis of subtracted PET images. *J Cereb Blood Flow Metab* 1988; 8:642-653.
18. Bergström M, Boëthius J, Eriksson L, Greitz T, Ribbe T, Widén L. Head fixation device for reproducible position alignment in transmission CT and positron emission tomography. *J Comput Assist Tomogr* 1981; 5:136-141.
19. Fox PT, Perlmutter JS, Raichle ME. A stereotactic method of anatomical localization for positron emission tomography. *J Comput Assist Tomogr* 1985; 9:141-153.